

Deploying Galactic Radio Explorer (GReX) Harvard Terminal: The All-Sky Search for Fast Radio Bursts from Magnetars

Larom Segev,^{1, a)} Liam Connor,¹ Sashabaw Niedbalski,² and Kiran Shila³

¹*Harvard University, Center for Astrophysics | Harvard & Smithsonian 60 Garden St., Cambridge, Massachusetts 02138, USA*

²*Cornell University, Department of Astronomy Space Sciences Building, Ithaca, New York 14853, USA*

³*California Institute of Technology, Cahill Center for Astronomy and Astrophysics, 1216 E. California Blvd., Pasadena, California 91125, USA*

^{a)}Corresponding author: laromsegev@college.harvard.edu

Abstract. Galactic Radio Explorer (GReX) is an all-sky radio monitor designed to detect the brightest fast radio bursts (FRBs) from undiscovered galactic magnetars and allow us to study their broadband emission. Building on STARE2's success, GReX features 1.3–1.5 GHz feeds and high-performance, low-noise amplifiers, allowing for ~ 10 -ms resolution. A unit was deployed at Harvard, with plans for global expansion to achieve continuous 4π steradian coverage. This work details the integration and modeling of GReX components, including server-network setup, dish-box connections, and initial tests across sites. The system temperature T_{sys} was calculated at ~ 51 K, corresponding to a projected detection rate of 6 FRBs/year. Site-specific radio frequency interference levels were assessed, revealing $\sim 17.4\%$ or 10 dBm higher interference at the Science and Engineering Complex compared to the Center for Astrophysics (CfA), leading to our selection of the CfA for installation. The telescope is fully operational, monitoring for FRB signals.

INTRODUCTION

Fast radio bursts (FRBs) are millisecond-duration transient radio pulses whose origins have interested the astronomical community since their discovery in 2007 [1]. The pulses have incredibly high radio fluxes (~ 1 Jy at GHz frequencies) of different burst morphology and spectra [2], releasing as much energy in a millisecond as the Sun does in 80 years.

By measuring the arrival times of the burst at different frequencies, one can also determine the total amount of gas that the burst passed through, a quantity known as dispersion measure. Dispersion measures follow a $\Delta t \propto \lambda^2$, indicating propagation through an ionized medium, but the observed dispersion measures were significantly larger than those expected from galactic sources, strongly suggesting an extragalactic origin and traversal through the intergalactic medium (IGM) [3, 4]. More detections, including the first recurring FRB [5], ruled out cataclysmic origin models.

Arrays of telescopes which use interferometry, combining signals from multiple, widely separated receivers to get higher angular resolution than possible with single-dish telescopes, allow for the origin of FRB signals to be pinpointed [4]. CHIME and STARE2 localized FRB 200428, the first to be coming from *within* our Milky Way galaxy, to the known magnetar SGR 1935+2154, a type of neutron star with an extremely powerful magnetic field [6, 7].

However, the exact mechanisms within magnetars that produce these brief-duration (< 1 ms) and incredibly high radio fluxes (~ 1 Jy at GHz frequencies) of different burst morphology and spectra remain unknown [2, 8]. With their dispersion measures indicating redshifts of $z = 0.3$ – 1 and the most distant to date detected from 13 billion light years away [3], FRBs help characterize the IGM and free electron distribution [9] and could yield valuable insights into galaxy evolution and stellar remnants, serving as powerful probes of the universe [10, 11]. There is also an implied high all-sky event rate of FRBs, with detectable bursts happening around once per minute, suggesting that wide-field radio telescopes will be capable of detecting multiple FRBs per day and yielding catalogs crucial to the field [3].

THE DESIGN OF GREX

The Galactic Radio Explorer (GReX) builds upon the Survey for Transient Astronomical Radio Emission 2 (STARE2) concept [7], which pioneered a low-cost, three-station radio network in California to detect bright (multi-MJy) transients at 1.4 GHz. While STARE2 demonstrated the feasibility of detecting galactic FRBs with \sim kJy sensitivity, GReX significantly improves the design through enhanced sensitivity (sub-MJy) and a global network of antennas for continuous galactic plane monitoring. This advancement enables GReX to detect nearby, ultrabright bursts that could elucidate the connection between magnetars and FRBs.

GReX complements deep, high-resolution surveys by functioning analogously to x-ray all-sky monitors, providing

continuous coverage for \sim MJy bursts within the galactic plane. Its globally dispersed antennas enhance detection rates cost effectively, while low-noise amplifiers enable subband searches to probe FRB activity and emission mechanisms. Beyond FRBs, GReX is designed to detect super-giant pulses (SGPs) from pulsars with fluences exceeding $1 \text{ MJy } \mu\text{s}$ [12]. These extreme pulses probe the nonlinear plasma physics of pulsar magnetospheres [13, 14], testing coherent emission mechanisms at energy densities approaching the Schwinger limit ($\sim 10^{18} \text{ V/m}$), magnetospheric particle acceleration beyond standard polar cap/slot gap models [15], and plasma turbulence scales where quantum electrodynamics (QED) effects may dominate classical electrodynamics [16]. Such detections could reveal whether SGP emission shares physical processes with FRBs from galactic magnetars [11].

The GReX instrument employs a modular design, integrating a cakepan dish feed connected to two low-noise amplifiers (LNAs) for horizontal and vertical polarizations to the box containing much of the signal processing. The front-end module (FEM) filters, amplifies, and down converts the signals, which are then digitized by a Smart Network ADC processor (SNAP). A Raspberry Pi facilitates monitor and control functions, while a GPS-synchronized oscillator provides a stable 10-MHz reference. Data is transmitted to a server running a multitiered pipeline. These pipeline stages include T0 (raw data capture), T1 (real-time RFI mitigation and dedispersion), T2 (offline, computationally intensive processing), and T3 (source extraction and visualization). The GReX pipeline leverages Docker containers for consistent and easy deployment across stations. A station at Harvard provides additional sky coverage and overlaps with the field of view of the already on-sky Cornell GReX terminal, enabling cross-correlation of signals to confirm detection of a flagged FRB candidate. These two stations also work alongside the first GReX station at Owens Valley Radio Observatory (OVRO) and an on-sky station at Trinity College Dublin.

INSTRUMENTATION ASSEMBLY AND SOFTWARE SETUP

The GReX deployment at Harvard University involved the integration of several hardware and software components. The GReX box, containing the FEM, SNAP, Raspberry Pi, and GPS-synchronized oscillator, was connected to the "cake-pan" dish antenna. Coaxial cables linked the dual-polarization feeds to the LNAs. The system was connected to a server via a 10-GbE fiber link. Key software setup steps included configuring the operating system on the server and Pi, establishing network connections using dnsmasq for static IP assignments, and installing the CUDA toolkit and necessary software dependencies (PSRDADA, heimdall-astro). The GReX pipeline was then deployed, with Grafana used for monitoring system performance (Fig. 1).



FIGURE 1. Grafana dashboard displaying live systematics and data coming from GReX.

RADIO FREQUENCY INTERFERENCE TESTS

Radio frequency interference (RFI) tests characterize the level of unwanted signals present at a potential observation site. These tests help identify and quantify sources of interference that could obscure or mimic faint signals. RFI tests involve measuring the power levels across and immediately surrounding the frequency range of interest using a spectrum analyzer connected to an antenna. In our case, we scanned from 1 to 1.8 GHz, using the dish antenna, LNA, bias tee, and spectrum analyzer to identify RFI sources at potential sites. We assessed the Center for Astrophysics (CfA) and the Science and Engineering Complex (SEC) at Harvard, finding that the CfA exhibited significantly lower

RFI levels, particularly near the edges of our frequency band (Fig. 2). Given the lesser fluctuations at RFI hotspots, the Harvard GReX unit was installed at the CfA to maximize the signal-to-noise ratio for FRB detection. We are actively exploring Oak Ridge Observatory as the potential long-term, future location due to its anticipated lower RFI levels, as it is located nearby for maintenance, yet in a rural and radio-quiet region of Massachusetts.

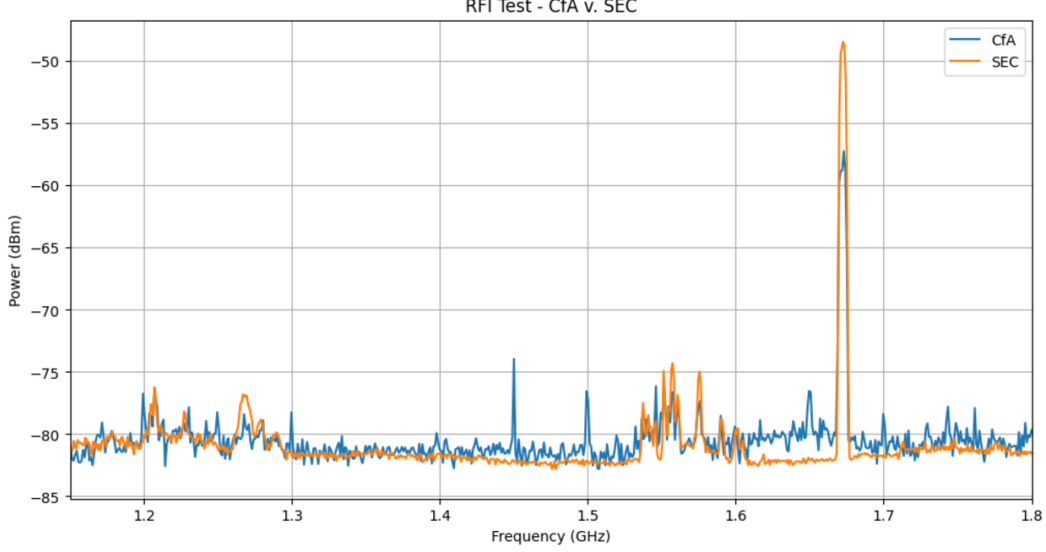


FIGURE 2. Spectral comparison of RFI at the SEC (orange) and CfA (blue). The SEC exhibits RFI fluctuations of greater magnitude at the majority of the locations of persistent interference.

SYSTEM TEMPERATURE MEASUREMENT

To characterize the system noise performance, we performed hot/cold load tests to measure the system temperature (T_{sys}). This method involves comparing the power received from a hot load (ambient temperature RF foam popsicle) and a cold load (liquid-nitrogen-cooled RF foam popsicle). Prior to T_{sys} measurements, we confirmed the consistent operation of both LNAs by comparing their signal power across frequency under identical conditions. Data was recorded with the antenna pointed at the sky, capturing the cosmic microwave background (CMB) and synchrotron radiation, and then with the antenna covered by a liquid-nitrogen-cooled absorber. The Y -factor, defined as the dimensionless ratio of the sky signal to the cold load signal (accounting for the logarithmic power scale), is calculated as

$$Y = A_{sky} - A_{cold}, \quad (1)$$

where A represents the measured amplitude. The system temperature is then calculated using

$$T_{sys} = \frac{T_{hot} - Y \cdot T_{cold}}{Y - 1}. \quad (2)$$

Here, T_{hot} is the ambient temperature (295 K), and T_{cold} is the temperature of liquid nitrogen (80 K). Our measurements yielded an average T_{sys} of 50.9 K, with a parabolic frequency dependence showing the lowest system temperature within the GReX frequency band (Fig. 3). This is around what is expected, given the first station, set up at the radio-quiet Owens Valley Radio Observatory, had a system temperature average baseline of ~ 36 K, and the Harvard terminal is expected to pick up on more RFI from the city surrounding it.

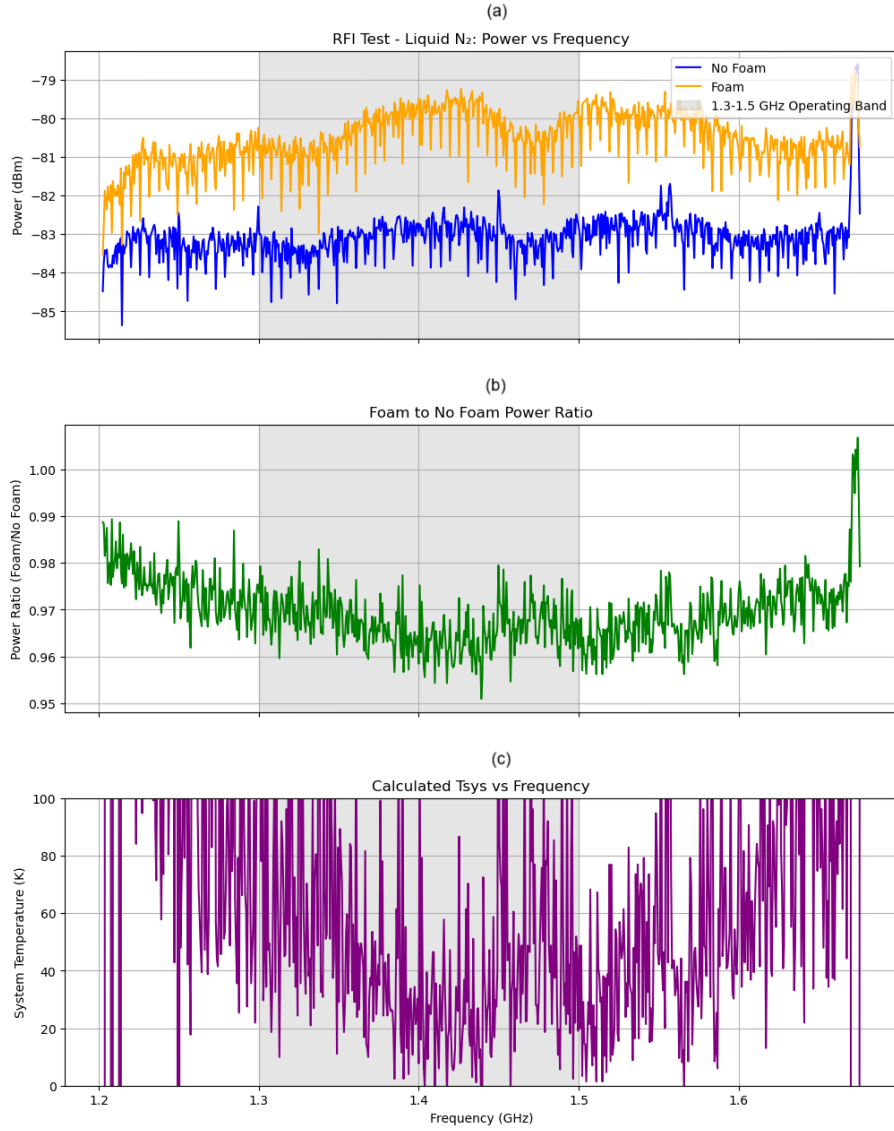


FIGURE 3. (a) The raw power signal captures when liquid nitrogen-cooled foam was covering it (blue) versus when it was pointed at the sky capturing CMB synchrotron radiation (orange). (b) The Y factors, a ratio of the power signals accounting for the log power scale. (c) The calculated T_{sys} across frequency.

SIGNAL INJECTION TESTS

The Harvard GRex pipeline successfully identifies FRB candidates when telltale signatures are injected into the data stream, demonstrating its end-to-end functionality and readiness for real-time FRB detection (Fig. 4). This validation process involves artificially inserting FRB-like signals with known characteristics (e.g., dispersion measure, burst width, and intensity) into the data stream at various points in the pipeline. This allows us to validate that the pipeline is operational and fully able to accurately and reliably alert the team to any potential FRBs it detects in real time.

The pipeline has a high completeness and is able to detect and characterize the burst properties of $\sim 95\%$ of the injected FRBs. The system can detect 1-ms bursts with flux density ≥ 50 kJy at a signal-to-noise ratio (SNR) of 10 when the source is at beam center, with sensitivity decreasing for off-center sources and scaling inversely with the square root of burst duration [17].

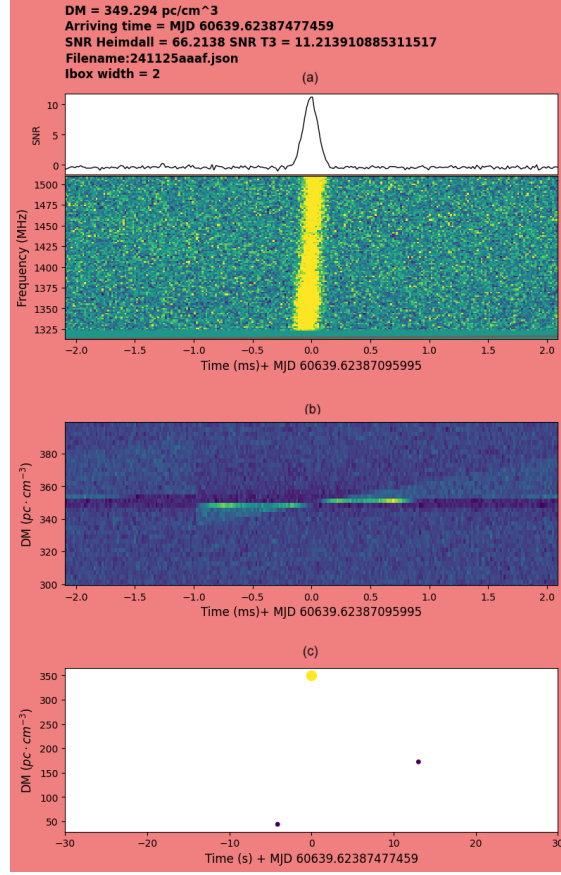


FIGURE 4. Automated notification of the first injected FRB signal that Harvard GReX successfully flagged. (a) The distribution of SNR against time. (b) The dark matter (DM) distribution of the detected signal. (c) The relationship between time and DM, with point sizes proportional to SNR. These plots collectively facilitate the analysis and verification of detected FRB signals such as the one flagged here.

MODELING FIELD OF VIEW AND DETECTION CAPABILITIES

Based on its measured system temperature (T_{sys}) and scaling the detection rate of STARE-2 [7], GReX is projected to have a detection rate of approximately 6.76 FRBs per year (Fig. 5). The detection rate of a station is modeled by the equation

$$\text{Rate} = \omega \cdot \Omega \cdot \left(\frac{\text{Gain}}{T_{\text{sys}}} \cdot \sqrt{B \cdot n_{\text{pol}}} \right)^{\alpha}, \quad (3)$$

where FRBs per year ω is the intrinsic event rate, Ω is the field of view (beam solid angle) of the telescope, $\text{Gain} = 0.7$ KJ/year is the telescope gain, T_{sys} is the system temperature, B is the bandwidth, $n_{\text{pol}} = 2$ is the number of polarizations, and $\alpha = 1.5$ is the spectral index for many radio transients.

While this detection rate may initially seem low, this is the rate of a single, high-RFI station, and the goal is to have an array of GReX stations working together, which boosts total detection rate with each station added. To achieve full 4π steradian coverage, 24/7, GReX aims to establish stations at universities worldwide, with a particular interest in rural low-RFI sites in the Southern and Eastern Hemispheres. We are evaluating the potential of setting up a new GReX station at the University of South Alabama using existing components at Caltech, which is expected to significantly enhance coverage at higher hour angles until more Southern Hemisphere stations are deployed (Fig. 6). The magnetar fraction, or the fraction of the sky or time during which galactic magnetars are within the field of view (FoV) of the GReX telescope array, is determined by location-specific latitude and longitude. The total magnetar fraction for a multistation GReX array is determined by summing the magnetar fraction of each individual station. The

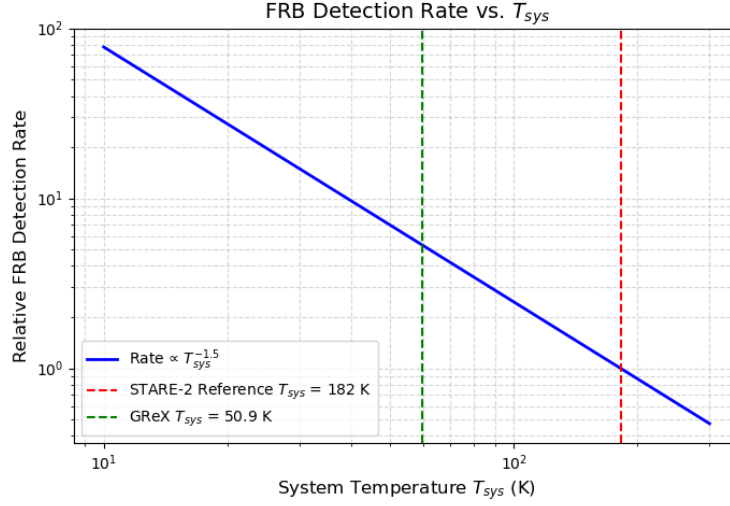


FIGURE 5. Plot showing predicted GReX detection rate where the GReX system temperature (dotted red line) intersects the model of how detection rate depends on system temperature (solid blue line).

beam coverage of each station is depicted in (Fig. 7), overlaid on a distribution of known magnetars and galactic plane emission, highlighting how much each station contributes, the need for more stations in the Southern Hemisphere, and the potential of more stations pushing the network to all-sky.

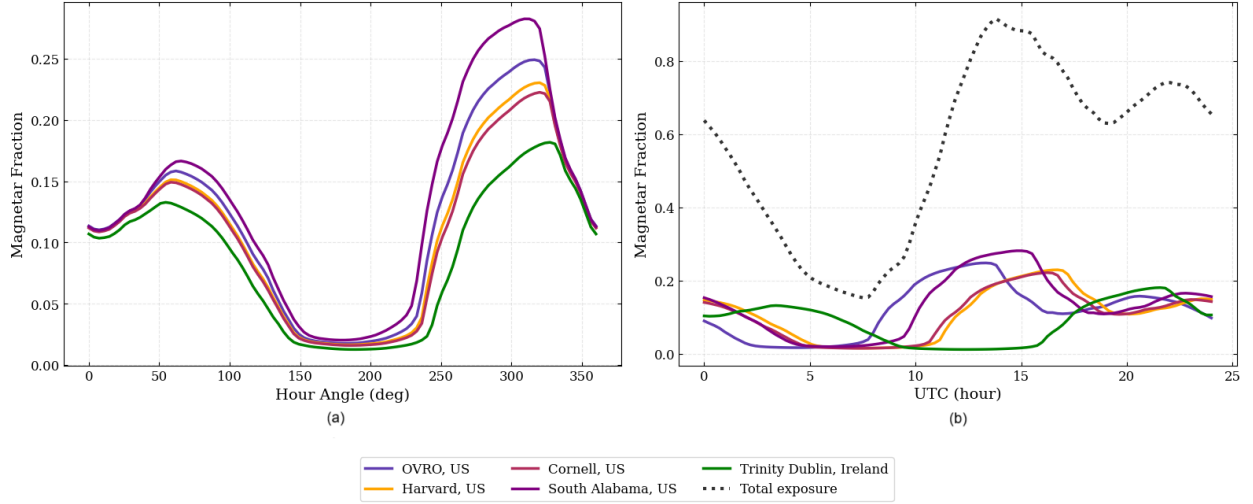


FIGURE 6. Galactic magnetar fraction modeling within the FoV given the present and proposed GReX locations around the world. (a) Magnetar fraction as a function of hour angle. (b) Magnetar fraction as a function of UTC, which accounts for the fact that each location sees only certain right ascension at a given time of day. The dotted line is the summed visible fraction of the GReX array.

CONCLUSIONS

The GReX station at Harvard University has been successfully deployed and is operational, searching for bright, nearby FRBs. With a measured system temperature (T_{sys}) of 50.9 K, the Harvard GReX is projected to detect approximately 6 FRBs per year. Future work includes exploring the quieter radio environment of Oak Ridge Observatory,

All-Sky Magnetar Distribution with Station Coverage

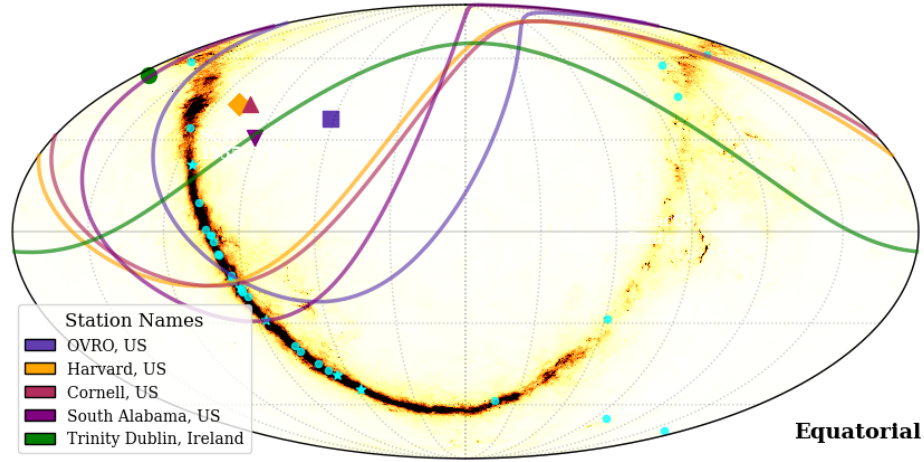


FIGURE 7. All-sky distribution of known magnetars overlaid on the Planck 857 GHz sky map in galactic coordinates. Magnetar positions are marked in cyan, with radio-emitting sources indicated by stars and non-radio sources by circles. Beam coverage regions ($\sim 120^\circ$ full width at half maximum) from five observing stations—OVRO (USA), Harvard (USA), Cornell (USA), South Alabama (USA), and Trinity College Dublin (Ireland)—are shown as colored contours. The galactic center and SGR 1935+2154 are labeled for reference. Background map intensity corresponds to far-infrared dust emission from the Planck survey. This figure highlights the global coverage and detection potential of a distributed magnetar monitoring network.

which presents the potential for reduced RFI and improved sensitivity. The ultimate goal is to deploy more GREX stations for a global network of stations that has continuous, all-sky monitoring of the galactic plane for FRBs.

ACKNOWLEDGMENTS

Special thanks to Nimesh Patel and Daniel Sheen for helping with several of the RFI tests and feedback on this paper. Also, thank you to Gulirano Almuratova, Hannah Burrows, Callie García, and Casey Murray for their assistance in transporting equipment.

We use the *GNU Parallel* [18], *Astropy* [19], [20], [21], *HEALPix* [22], *PSRDADA* [23], and *HEIMDALL* [24] for data processing.

REFERENCES

1. D. R. Lorimer, M. Bailes, M. A. McLaughlin, D. J. Narkevic, and F. Crawford, “A bright millisecond radio burst of extragalactic origin,” *Science* **318**, 777–780 (2007).
2. E. Petroff, J. W. T. Hessels, and D. R. Lorimer, “Fast radio bursts at the dawn of the 2020s,” *Astron. Astrophys. Rev.* **30** (2022), 10.1007/s00159-022-00139-w.
3. E. Petroff, J. W. T. Hessels, and D. R. Lorimer, “Fast radio bursts,” *Astron. Astrophys. Rev.* **27** (2019), 10.1007/s00159-019-0116-6.
4. K. W. Bannister, A. T. Deller, C. Phillips, J.-P. Macquart, J. X. Prochaska, N. Tejos, S. D. Ryder, E. M. Sadler, R. M. Shannon, Simha, *et al.*, “A single fast radio burst localized to a massive galaxy at cosmological distance,” *Science* **365**, 565–570 (2019).
5. L. G. Spitler, P. Scholz, J. W. T. Hessels, S. Bogdanov, A. Brazier, F. Camilo, S. Chatterjee, J. M. Cordes, F. Crawford, J. Deneva, *et al.*, “A repeating fast radio burst,” *Nature* **531**, 202–205 (2016).
6. B. Andersen, K. Bandura, M. Bhardwaj, A. Bij, M. Boyce, P. Boyle, C. Brar, T. Cassanelli, P. Chawla, T. Chen, *et al.*, “A bright millisecond-duration radio burst from a galactic magnetar,” *Nature* **587**, 54–58 (2020).
7. C. D. Bochenek, V. Ravi, K. V. Belov, G. Hallinan, J. Kocz, S. R. Kulkarni, and D. L. McKenna, “A fast radio burst associated with a galactic magnetar,” *Nature* **587**, 59–62 (2020).
8. D. R. Lorimer, M. A. McLaughlin, and M. Bailes, “The discovery and significance of fast radio bursts,” *Astrophys. Space Sci.* **369** (2024), 10.1007/s10509-024-04322-6.
9. J.-P. Macquart, J. X. Prochaska, M. McQuinn, K. W. Bannister, S. Bhandari, C. K. Day, A. T. Deller, R. D. Ekers, C. W. James, L. Marnoch, *et al.*, “A census of baryons in the universe from localized fast radio bursts,” *Nature* **581**, 391–395 (2020).

10. M. P. Snelders, K. Nimmo, J. W. T. Hessels, Z. Bensellam, L. P. Zwaan, P. Chawla, O. S. Ould-Boukattine, F. Kirsten, J. T. Faber, and V. Gajjar, “Detection of ultra-fast radio bursts from FRB 20121102a,” *Nat. Astron.* **7**, 1486–1496 (2023).
11. B. Zhang, “The physics of fast radio bursts,” *Rev. Mod. Phys.* **95** (2023), 10.1103/revmodphys.95.035005.
12. L. Connor, K. A. Shila, S. R. Kulkarni, J. Flygare, G. Hallinan, D. Li, W. Lu, V. Ravi, and S. Weinreb, “Galactic radio explorer: An all-sky monitor for bright radio bursts,” *Pub. Astron. Soc. Pac.* **133**, 075001 (2021).
13. D. B. Melrose, “Coherent emission mechanisms in astrophysical plasmas,” *Rev. Mod. Plasma Phys.* **28**, 1–50 (2004).
14. M. Lyutikov, “Fast radio bursts as giant pulses from young rapidly rotating pulsars,” *Mon. Not. R. Astron. Soc.* **483**, 2766–2783 (2019).
15. J. M. Cordes and I. I. Wasserman, “Supergiant pulses from extragalactic neutron stars,” *Mon. Not. R. Astron. Soc.* **457**, 232–257 (2016).
16. D. A. Uzdensky and S. Rightley, “Plasma physics of extreme astrophysical environments,” *Rep. Prog. Phys.* **77**, 036902 (2014).
17. K. A. Shila, S. Niedbalski, L. Connor, S. R. Kulkarni, L. Segev, P. Shukla, E. F. Keane, J. McCauley, O. A. Johnson, B. Watters, *et al.*, “GReX: An instrument overview and new upper limits on the galactic FRB population,” (2025), arXiv:2504.18680 [astro-ph.HE].
18. O. Tange, “GNU parallel 20250222 (‘Grete Tange’),” (2025), 10.5281/zenodo.14911163.
19. Astropy Collaboration, T. P. Robitaille, E. J. Tollerud, P. Greenfield, M. Droettboom, E. Bray, T. Aldcroft, M. Davis, A. Ginsburg, A. M. Price-Whelan, *et al.*, “Astropy: A community Python package for astronomy,” *Astron. Astrophys.* **558**, A33 (2013), arXiv:1307.6212 [astro-ph.IM].
20. Astropy Collaboration, A. M. Price-Whelan, B. M. Sipőcz, H. M. Günther, P. L. Lim, S. M. Crawford, S. Conseil, D. L. Shupe, M. W. Craig, N. Dencheva, *et al.*, “The Astropy Project: Building an open-science project and status of the v2.0 core package,” *Astron. J.* **156**, 123 (2018), arXiv:1801.02634 [astro-ph.IM].
21. Astropy Collaboration, A. M. Price-Whelan, P. L. Lim, N. Earl, N. Starkman, L. Bradley, D. L. Shupe, A. A. Patil, L. Corrales, C. E. Brasseur, *et al.*, “The Astropy Project: Sustaining and growing a community-oriented open-source project and the latest major release (v5.0) of the core package,” *Astrophys. J.* **935**, 167 (2022), arXiv:2206.14220 [astro-ph.IM].
22. K. M. Górski, E. Hivon, A. J. Banday, B. D. Wandelt, F. K. Hansen, M. Reinecke, and M. Bartelmann, “HEALPix: A framework for high-resolution discretization and fast analysis of data distributed on the sphere,” *Astrophys. J.* **622**, 759–771 (2005), arXiv:astro-ph/0409513 [astro-ph].
23. W. van Straten, A. Jameson, and S. Osłowski, “PSRDADA: Distributed Acquisition and Data Analysis for Radio Astronomy,” *Astrophysics Source Code Library*, ascl:2110.003 (2021).
24. B. R. Barsdell, M. Bailes, D. G. Barnes, and C. J. Fluke, “Accelerating incoherent dedispersion,” *Mon. Not. R. Astron. Soc.* **422**, 379–392 (2012).